iScience

Article

A central role for Numb/Nbl in multiple Shh-mediated axon repulsion processes

Graphical abstract

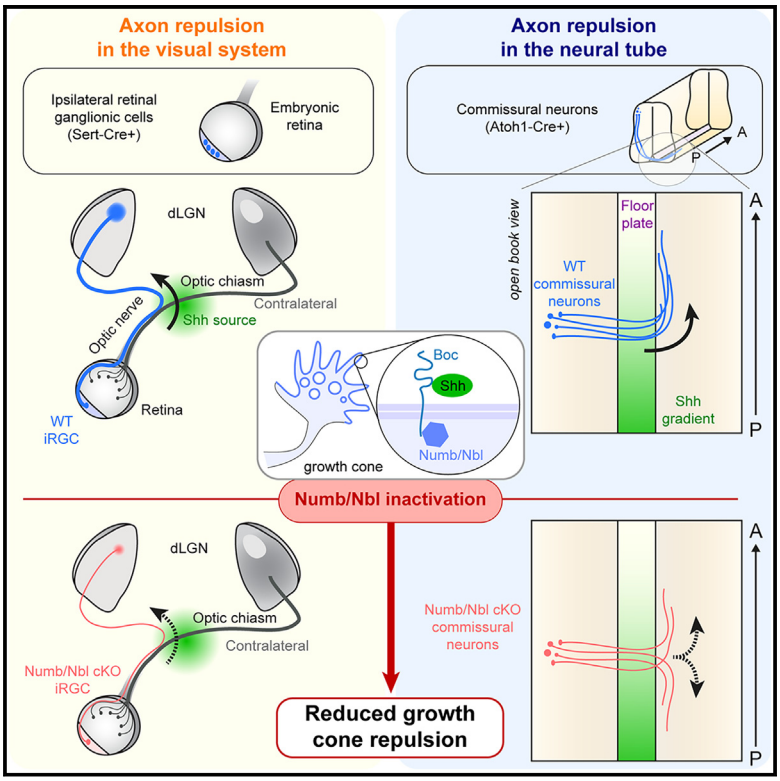

Highlights

- Conditional Numb/Nbl KO (cKO) in iRGCs leads to axonal segregation defects at the optic chiasm
- Shh-mediated growth cone collapse in iRGCs is dependent on Numb/Nbl
- Numb/Nbl cKO in commissural neurons results in spinal cord midline post-crossing defects
- Numb/Nbl is required for two distinct axon guidance repulsion processes involving Shh

Authors

Tiphaine Dolique, Sarah Baudet, Frederic Charron, Julien Ferent

Correspondence

frederic.charron@ircm.qc.ca (F.C.), julien.ferent@inserm.fr (J.F.)

In brief

Molecular biology; Neuroscience

Dolique et al., 2025, iScience *28*, 112293
May 16, 2025
https://doi.org/10.1016/j.isci.2025.112293

CellPress

iScience

CellPress
OPEN ACCESS

Article

A central role for Numb/Nbl in multiple Shh-mediated axon repulsion processes

Tiphaine Dolique,[1,2,4,8] Sarah Baudet,[5,6,7,8] Frederic Charron,[1,2,3,*] and Julien Ferent[1,5,6,7,9,*]
[1]Montreal Clinical Research Institute (IRCM), 110 Pine Avenue West, Montreal, QC H2W 1R7, Canada
[2]Department of Anatomy and Cell Biology, Division of Experimental Medicine, McGill University, Montreal, QC H3A 0G4, Canada
[3]Department of Medicine, University of Montreal, Montreal QC H3T 1J4, Canada
[4]Inovarion, 75005 Paris, France
[5]Institut du Fer à Moulin, Inserm, Sorbonne Université, Paris, France
[6]Sorbonne Université, CNRS, Inserm, Center of Neuroscience Neuro-SU, 75005 Paris, France
[7]Sorbonne Université, CNRS, Inserm, Institut de Biologie Paris-Seine, IBPS, 75005 Paris, France
[8]These authors contributed equally
[9]Lead contact
*Correspondence: frederic.charron@ircm.qc.ca (F.C.), julien.ferent@inserm.fr (J.F.)
https://doi.org/10.1016/j.isci.2025.112293

SUMMARY

Sonic hedgehog (Shh) is an axon guidance molecule that can act as either a chemorepellent or a chemoattractant, depending on the neuron type and their developmental stage. In the developing spinal cord, Shh initially attracts commissural axons to the floor plate and later repels them after they cross the midline. In the developing visual system, Shh repels ipsilateral retinal ganglion cell (iRGC) axons at the optic chiasm. Although Shh requires the endocytic adaptor Numb for attraction of spinal commissural axons, the molecular mechanisms underlying Shh dual function in attraction and repulsion are still unclear. In this study, we show that Numb is essential for two Shh-mediated repulsion processes: iRGC axon repulsion at the optic chiasm and antero-posterior commissural axon repulsion in the spinal cord. Therefore, Numb is required for Shh-mediated attraction and repulsion. These results position Numb as a central player in the non-canonical Shh signaling pathway mediating axon repulsion.

INTRODUCTION

During embryogenesis, growing axons are guided to their targets by molecular guidance cues. Sensing these cues, whether they are repulsive or attractive, is essential for correct axon guidance and circuit formation.[1] Among the many guidance cues, Sonic hedgehog (Shh) is a critical molecule that can act as a chemorepellent or chemoattractant, depending on the neuron type and developmental stage. In the neural tube, Shh is initially responsible for the attraction of commissural axons to the floor plate, through the action of Smoothened (Smo), β-arrestins, Src family kinases, and the WAVE regulatory complex.[2–6] After they have crossed the midline, Shh repels commissural axons along the antero-posterior axis.[7]

In the developing chick visual system, a species devoid of binocular vision, Shh is a chemorepulsive cue for retinal ganglion cell (RGC) axons.[8] In species with binocular vision, RGCs can either project to the same side of the brain (ipsilateral, iRGC) or to the opposite side (contralateral, cRGC). The segregation of these two types of RGCs occurs at the level of the optic chiasm and is controlled by the repulsion of iRGCs by Ephrins (through their Eph receptors) and by Shh (through its receptor Boc).[9–14] Shh is produced by cRGCs in the retina and is then transported anterogradely along the axon.[15] Shh accumulates at the optic chiasm and induces repulsion of iRGCs via an axon-axon interaction mechanism.

Receptors are targeted to specific sites on the cell membrane through endocytosis and/or exocytosis, a mechanism essential for axon guidance.[16–19] We have previously shown that Shh-mediated Boc endocytosis is required for the attraction of commissural axons in the developing spinal cord.[20] Both Shh attraction and Boc internalization are dependent on the endocytic membrane-associated protein Numb. Numb is a polarized fate determinant during asymmetric cell division in vertebrates and Drosophila.[21,22] During mammalian neurogenesis, Numb and its homolog Numb-like are critical for maintaining neural progenitor cells by ensuring that these cells prefer progenitor over neuronal fates, preventing depletion of dividing cells, and ensuring proper neural development.[23,24] It is also required for the migration of cerebellar progenitors via polarized endocytosis of several receptors, including TrkB and integrins.[25,26] In hippocampal neurons, neurite outgrowth has been shown to depend on the interaction of Numb and the L1 receptor.[27] At the level of the retina, Numb is required to generate terminal asymmetric cell divisions and regulates the polarized delivery of cyclic nucleotide-gated ion channels in rod photoreceptor cilia.[28,29] However, it is unknown whether the function of Numb in Shh signaling is conserved in other non-canonical Shh responses such as axonal repulsion.

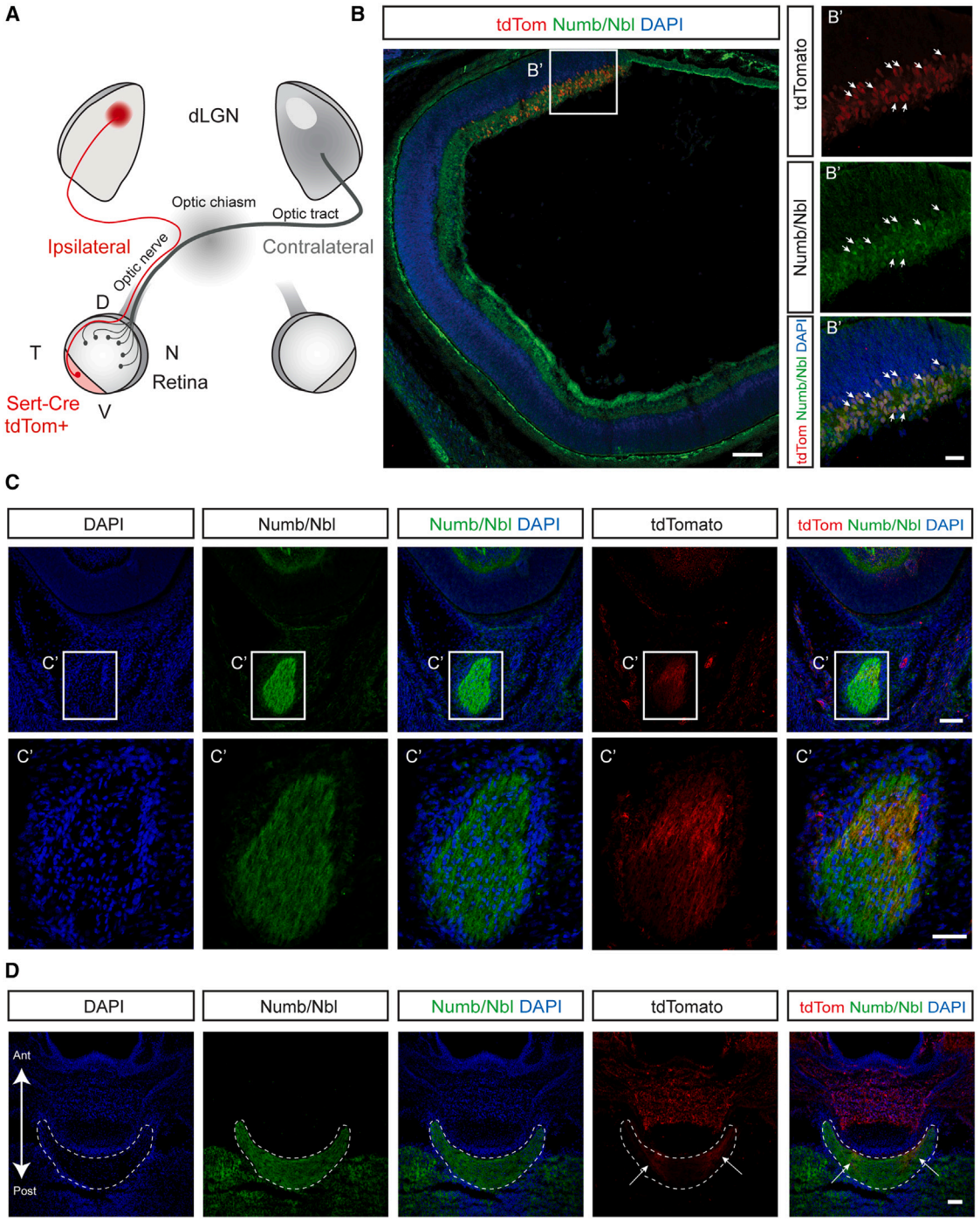

Figure 1. Numb/Nbl is expressed by iRGCs

(A) Schematic showing the organization of RGC projections from the retina to the dLGN and the distribution of tdTomato expressed under the Sert-Cre driver.

(B) Mouse P0 Sert-Cre; Rosa26-tdTomato retina sections immunostained for Numb/Nbl. (B′) Enlargement of the retinal ventrotemporal region where tdTomato$^+$ cells are found. Neurons positive for both tdTomato and Numb/Nbl are indicated by white arrows.

(legend continued on next page)

Therefore, we investigated whether Numb is essential for axon repulsion in two different systems where Shh acts as a repulsive cue: the segregation of ipsilaterally-projecting RGC axons at the optic chiasm and the antero-posterior repulsion of post-crossing commissural axons after they have crossed the neural tube midline.

RESULTS

Numb and Nbl are expressed in iRGCs

Numb and its homolog Numb-like (Nbl) are expressed broadly in the developing nervous system[22] and can be functionally redundant.[23] We examined the expression of Numb and Nbl in the retina using an antibody that recognizes both proteins.[28] Numb/Nbl expression has been described in the RGC layer,[28] but it is unknown whether it is expressed by iRGCs. To specifically label iRGCs, we used a Cre recombinase under the control of the Slc6a4 promoter (serotonin transporter; Sert-Cre) to activate the expression of the tdTomato reporter gene (Figure 1A).[15,30] In the retina of postnatal day 0 (P0) mouse, tdTomato$^+$ cells are restricted to the ventrotemporal region, where iRGCs are located (Figures 1B and B'). Numb/Nbl expression appears high throughout the retina, especially in the RGC layer (Figure 1B). We detected a strong colocalization of Numb/Nbl with tdTomato$^+$ cells (Figure 1B'), demonstrating robust expression of Numb/Nbl by iRGCs. We observed that Numb/Nbl signal is also very high in the optic nerve and at the optic chiasm (Figures 1C and 1D). In addition to labeling cell bodies, the tdTomato signal allows visualization of iRGC axons along the entire optic pathway. Colocalization of Numb/Nbl and tdTomato is also high in axons in the optic nerve and chiasm (Figure 1C', D). Axonal localization of Numb/Nbl has also been observed in other types of neurons, such as hippocampal neurons[27] or spinal commissural neurons,[20] suggesting that Numb/Nbl may also play a role at a distance from the cell bodies of iRGCs.

Numb/Nbl iRGC conditional knock-out does not affect eye morphology and iRGC specification

When *Numb* and *Nbl* are deleted in the early retina, eye development is severely disrupted.[28] Mutant eyes are hypoplastic and the number of most retinal cell types is reduced.[28] To investigate the role of Numb and Nbl specifically in iRGC and avoid the retinal structural defects caused by early deletion of *Numb* and *Nbl*, we used the Sert-Cre mouse line to inactivate conditional alleles of *Numb* and *Nbl*.[31] We refer to the resulting conditional mutants as Sert-Cre cDKO. We next verified the decrease of Numb/Nbl immunoreactivity in the ventrotemporal regions of the Sert-Cre cDKO mutant retinas, where the iRGCs reside (Figure S1). Numb/Nbl immunoreactivity shows strong vesicular-like structure in the cell body of RGCs, as previously described.[32] This signal is reduced in the ventrotemporal retina but not in the dorsomedial retina of Sert-Cre cDKO, indicating the spatial specificity of the KO. The structure of the eyes of P0 Sert-Cre cDKOs was analyzed in comparison to control littermate animals. Measurements of several parameters including eye diameter, eye area, retinal area, optic nerve and optic tract area showed no differences between Sert-Cre cDKO and controls (Figures 2A–2F). Thus, conditional knockout of *Numb* and *Nbl* in iRGCs does not affect the gross anatomy and morphological measurements of the eye and its projection.

Since early deletion of Numb/Nbl in retinal progenitors showed that Numb/Nbl are required for the normal production of retinal cell types,[28] we next examined whether iRGC specification and survival are affected in Sert-Cre cDKO. For this, we stained P0 retinal sections from control or Sert-Cre cDKO for Zic2, a transcription factor that specifies the ipsilateral fate of RGCs.[33] Quantification of the number of Zic2$^+$ cells showed no changes between controls and Sert-Cre cDKO (Figures 2G and 2H). We also looked in adults (3–4 months old) and observed that the number of Sert-Cre tdTomato$^+$ cells was not different between controls and Sert-Cre cDKO (Figures 2I and 2J), demonstrating that *Sert-cre* mediated Nb/Nbl inactivation does not affect the production or survival of iRGCs in the retina.

Numb/Nbl is required for ipsilateral axon segregation *in vivo*

iRGC axons are repelled at the level of the optic chiasm and thus ultimately project ipsilaterally to the thalamus. One of the guidance cues known to control this repulsion is Shh.[10] Shh is produced by cRGCs and transported along their axons to the optic chiasm where it repels iRGC axons locally.[15] This effect of Shh is mediated by its receptor Boc.[10] In the developing spinal cord, Shh-mediated chemoattraction of commissural axons also acts via Boc and requires Numb as an endocytic adaptor.[20] However, the molecular mechanism underlying the repulsion induced by Shh via Boc in iRGC growth cones remains unknown. Therefore, we wondered whether Numb/Nbl might also play a role in the repulsion of iRGC axons at the optic chiasm. To investigate the projections of ipsilateral axons from the eye to the brain, we injected DiI into one eye and quantified DiI fluorescence intensities in contralateral and ipsilateral optic tract sections at P0 (Figure 3A). Compared to the control, Sert-Cre cDKO resulted in a decrease in the ipsilateral fraction (control: 14.67% ± 0.67%, Sert-Cre cDKO: 10.94% ± 0.42%; $n \geq 4$ animals; $p = 0.0141$) (Figures 3B and 3C). To further characterize this decrease in the segregation of RGC axons at the chiasm, we examined the distribution of terminal projections in the dorsal lateral geniculate nucleus (dLGN) of the thalamus by whole-eye anterograde labeling using cholera toxin subunit B (CTB) coupled to fluorophores (Figure 3D). Since each eye is injected with a CTB conjugated to a different fluorophore, retinal axons can be labeled in an eye-specific manner and their projections analyzed in the dLGN (Figure 3E). Ipsilateral axons are shown in green and contralateral axons are shown in red. The fluorescence intensity of the ipsilateral projections was decreased in

(C) Optic nerve sections immunostained for Numb/Nbl. (C') Enlargement of the optic nerve section where tdTomato$^+$ axons are detected, together with Numb/Nbl staining.

(D) Optic chiasm sections (dotted line) immunostained for Numb/Nbl. The arrows show Sert-Cre; Rosa26-tdTomato$^+$ ipsilateral projections from the retina. Scale bars: 100 μm in (B); 25 μm in (B'); 100 μm in (C and C'); 100 μm in (D).

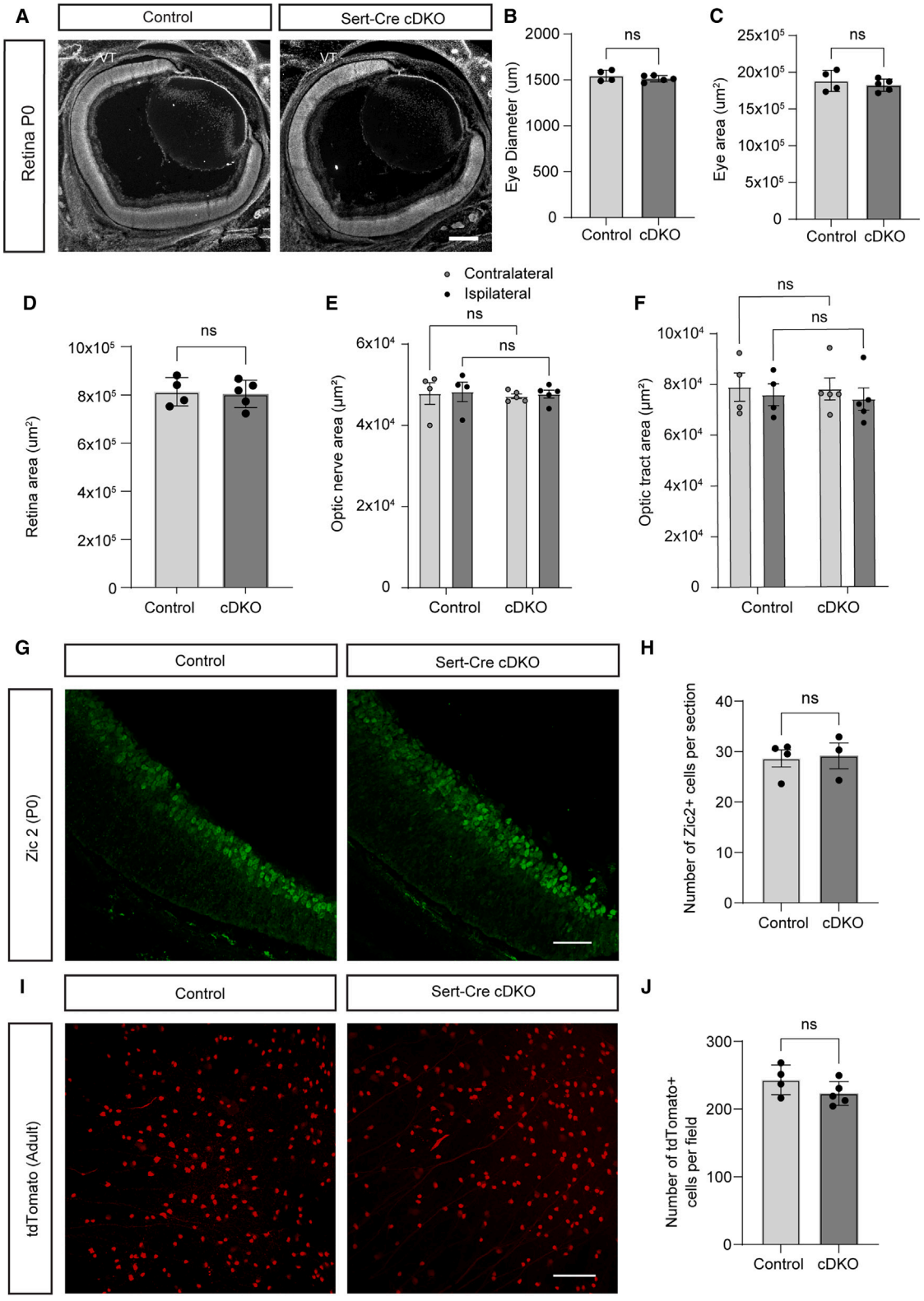

(legend on next page)

the dLGN of Sert-Cre cDKO compared to the control. This was confirmed by analyzing the percentage of the dLGN territory occupied by ipsilateral inputs. We performed this analysis using different fluorescence threshold (a method developed in the study by Rebsam et al.,[34] to ensure the robustness of the effect at multiple threshold intensities) and observed a consistent trend. For instance, when the ipsilateral detection threshold was set to 35, the percentage of dLGN area occupied by ipsilateral terminals showed a 36% decrease in Sert-Cre cDKO compared to controls (p = 0.0367, Figure 3F). This decrease goes up to 49% when the threshold was set at 30 (p = 0.0164, Figure 3F). Importantly, the contralateral input and the total dLGN area remained unchanged (Figures 3G and 3H). Overall, these result show that Numb/Nbl is required for the proper guidance of iRGC axons at the optic chiasm and for their final segregation in the dLGN.

Numb/Nbl is required for Shh-induced iRGCs growth cone collapse

To determine whether Numb is required for Shh-dependent repulsion in the context of iRGC axon guidance, we performed Shh-induced collapse assays on retinal explants. We knocked-down Numb and Nbl using shRNAs by electroporating the shRNA expression constructs into ex-utero E14.5 retina (Figure S2). Retinas were dissected and explants were grouped according to the orientation of the eye: ventro-temporal (VT) explants containing iRGCs were separated from non-VT explants containing all other regions. Immunostaining for SERT indicated the ipsilateral identity of the electroporated axons, which themselves were identified by GFP expression (GFP is expressed by the shRNA plasmid). The specificity of these staining was further validated by co-staining with an anti-Shh, which labels cRGCs and shows no colocalization with SERT (Figures S3A and S3B). Similar to what we showed previously, a 30-min stimulation with Shh induced a significant increase in the proportion of collapsed growth cones from iRGCs electroporated with a scrambled control plasmid.[10] Interestingly, this effect was blocked when Numb/Nbl were knocked-down (Figures 4A and 4B). We also analyzed non-electroporated growth cones from the same explants and confirmed that GFP-negative iRGCs retained their sensitivity to Shh, as the percentage of collapse of these growth cones increased in response to Shh (Figures 4C and 4D). To confirm the specificity of this effect, we performed a rescue experiment by co-expressing a shRNA-resistant form of Numb or Nbl ($Numb^{shResistant}$ or $Nbl^{shResistant}$), along with the Nb+Nbl shRNAs (Figures 4A and 4B). Collapse analysis showed that growth cones of neurons expressing either the resistant form of Numb or Nbl regain collapse when exposed to Shh, demonstrating that either Numb or Nbl is sufficient to mediate Shh-dependent collapse.

Together, these results demonstrate that Numb/Nbl are required for proper ipsilateral retinal projection segregation at the optic chiasm and for Shh-mediated collapse of iRGCs.

Numb/Nbl is required for post-midline crossing guidance in the developing spinal cord

In addition to the developing visual system, Shh also has a repulsive function in the developing spinal cord. After commissural axons reach the midline, they switch their sensitivity to Shh from attraction to repulsion.[7] Shh then acts as a repellent to make commissural axons turn anteriorly. Since Numb/Nbl is required for commissural axons to be initially attracted by Shh,[20] and that Numb/Nbl is also required for Shh-mediated repulsion in the visual system (this work), we wondered whether Numb/Nbl is also required for repulsion of commissural axons after midline crossing. We first examined the expression of Numb and Nbl in commissural neurons. Using commissural neurons isolated from E13.5 rat spinal cords and cultured for four days (4DIV), we performed immunostaining for Numb/Nbl and co-staining for filamentous actin (phalloidin). At 4DIV, commissural axons are repelled by Shh.[7] We showed that Numb/Nbl is present at the growth cone level in vesicle-like structures, in filopodia and in the axonal shaft (Figure 5A). RNA sequencing (RNA-seq)[35] revealed significant expression of Numb and Nbl in commissural neurons, similar to the levels of Ptch1 (Figure 5B), both at 2DIV, when axons are attracted to Shh, and at 4DIV, when they are repelled by Shh. Using mouse embryos at E11.5, we also stained for Numb/Nbl in tissue sections and for L1, a marker of post-crossing commissural axons (Figure 5C). We observed that L1 staining colocalizes with the Numb/Nbl signal. Taken together, this shows that Numb/Nbl, in addition to being expressed in pre-crossing commissural neurons,[20] is also highly expressed by commissural neurons after their axons have crossed the midline. Next, we investigated if Numb and Nbl are required for guidance after midline crossing. For this, we analyzed conditional mutant embryos in which Numb/Nbl is removed from dI1 commissural neurons by crossing *Nb; Nbl* floxed mice[31] with mice expressing the Atoh1-Cre driver.[36] Quantification of Nb/Nbl immunoreactivity in the ventro-medial funiculi (a zone where post-crossing commissural axons are located) revealed a significant decrease in the fluorescence intensity of the Numb/Nbl staining in the mutants compared to controls

Figure 2. Numb/Nbl cDKO in iRGCs does not affect eye morphology and iRGC specification

(A) Retina sections at P0 from control and Sert-Cre cDKO animals. The cell nuclei were stained with DAPI. The eye diameter (B), the eye area (C), the retina area (D), the optic nerve area (E), and the optic tract area (F) were measured and compared between control and Sert-Cre cDKOs and showed no significant differences.

(G) Retina sections from mouse P0 control or Sert-Cre cDKO were stained for Zic2.

(H) The number of $Zic2^+$ cells per section was not different between genotypes.

(I) Flat mount preparation of adult control or Sert-Cre cDKO retinas showing $tdTomato^+$ cells.

(J) The $tdTomato^+$ cell density shows no difference between control and Sert-Cre cDKO. Data are mean ± s.e.m and dots represent individual animals. Mann-Whitney tests were performed in (B, C, D, H and J). two-way ANOVA was performed in (E and F). ns. = not significant ($p > 0.05$). Scale bars: 250 μm in (A); 50 μm in (G); 100 μm in (I). See also Figure S1.

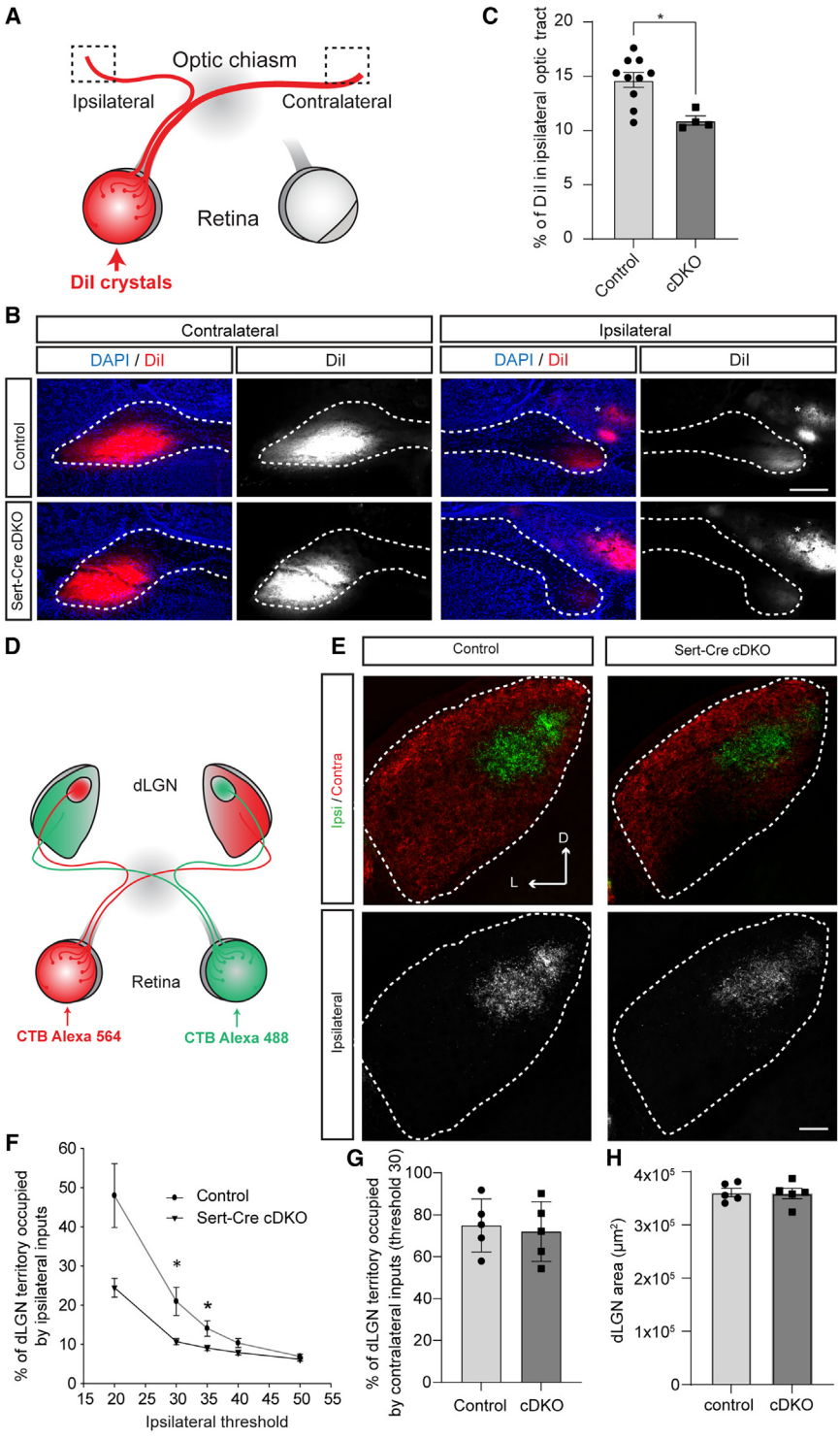

Figure 3. Numb/Nbl is required for ipsilateral axon segregation *in vivo*

(A) Scheme of the DiI injection protocol.

(B) Optic tract sections from P0 control and Sert-Cre cDKO animals injected with DiI. Dotted lines indicate the optic tract. The asterisk indicates a fluorescence artifact which always appears on the ipsilateral side of the injection.

(C) Decreased percentage of DiI fluorescence in Sert-Cre cDKO ipsilateral optic tract compared to controls (Mann-Whitney test, mean ± s.e.m, * = $p < 0.05$).

(D) Scheme of the CTB injection protocol.

(E) Retinogeniculate projections in control and Sert-Cre cDKO dLGN at the adult stage, with ipsilateral projections in green and contralateral projections in red. Binary images of ipsilateral projections are shown below.

(F) Percentage of ipsilateral segregated inputs in the dLGN as a function of threshold (3 sections were averaged per animal, $n = 5$ animals per genotype, Mann-Whitney test, mean ± s.e.m, * = $p < 0.05$).

(G) No difference in the percentage of contralateral segregated inputs in the dLGN analyzed with a threshold of 30 (Mann-Whitney test, mean ± s.e.m).

(H) No difference in dLGN area between control and Sert-Cre cDKO (Mann-Whitney test, mean ± s.e.m).

Scale bars: 200 µm in B; 100 µm in E

(Figure S4). The fluorescence intensity of L1 staining in Atoh1-Cre cDKOs did not change compared to controls (Figures 5D and 5E), nor did the thickness of the ventral commissures as measured by TAG1 immunostaining (Figures 5F and 5G). As we have previously shown with a ROBO3 staining,[20] this indicates that although the inactivation of Nb/Nbl induces guidance errors on the way to the midline, the majority of axons still end up reaching the floor plate. However, the consequences of Nb/Nbl deletion on the axons reaching the floor plate, which should be turning toward the anterior pole of the neural tube, remained to be determined. To assess the role of Numb/Nbl in antero-posterior guidance, we labeled commissural axons in E12.5 embryos with DiI. This technique visualizes the trajectory of commissural axons after crossing. We have previously validated our DiI injection protocol using an Atoh1-GFP transgene to localize the position of the Atoh1$^+$ cell bodies and the site of DiI injection.[7] Here, we observed a significant decrease in the ratio of anterior-guided axons to the total fluorescence of both anterior- and posterior-guided axons in the Atoh1-Cre cDKO compared to the controls (Figures 5H and 5I). This indicates an increase in misrouted axons that turn toward the posterior part of the neural tube in absence of Numb/Nbl. It is worth noting that this difference is similar to what we have previously observed in a conditional knock-out of Smoothened in commissural neurons.[7] Thus, our results reveal that Numb/Nbl play a

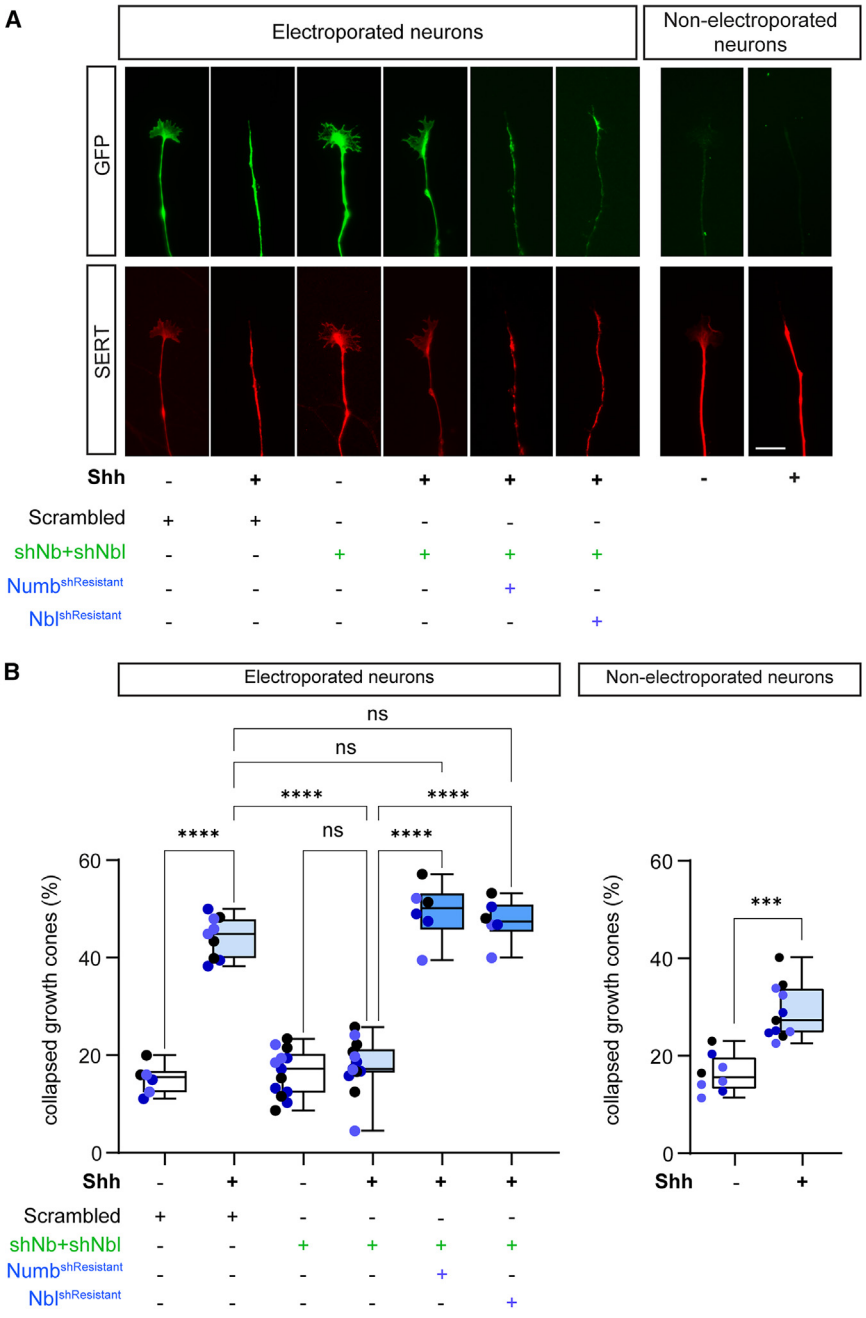

Figure 4. Numb/Nbl is required for Shh-induced iRGCs growth cone collapse

(A) iRGCs from ventro-temporal retina explants electroporated with scrambled or shNb and shNbl (green), and in combination or not with either a shRNA-resistant form of Numb (Numb^{shResistant}) or Nbl (Nbl^{shResistant}), identified by SERT immunostainings (red).

(B) Quantification of the percentage of electroporated iRGC collapse after Shh or control stimulation. One-way ANOVA and Tukey multiple comparison test, dots represent individual coverslips, with an average of 115 growth cones per coverslip quantified. Asterisks (*) indicate significance as follows: *** = $p < 0.001$, **** = $p < 0.0001$, ns. = not significant ($p > 0.05$). Each independent experiment is color-coded. Quantification of the percentage of non-electroporated iRGC collapse after Shh or control stimulation were also performed. Scale bars: 20μm in (A). See also Figure S2 and S3.

role in the guidance of post-crossing commissural axons along the longitudinal axis.

DISCUSSION

Our data indicate that the endocytic adaptors Numb/Nbl are required for repulsive axon guidance in two different neurodevelopmental systems: iRGC segregation in the visual system and antero-posterior guidance after midline crossing in the spinal cord. Since we previously showed that Numb/Nbl are required for Shh-mediated attraction of pre-crossing commissural axons in the developing spinal cord,[20] together, these results demonstrate that Numb/Nbl are involved in both repulsion and attraction.

In this study, we generated an ipsilateral RGC-specific KO of Numb/Nbl using Sert-Cre. In adult mice, we found no difference in the number of Sert-Cre tdTomato+ cells between control and Sert-Cre cDKO animals. This indicates that Sert-Cre-mediated inactivation of Numb/Nbl does not affect the generation of iRGCs in the retina. In contrast, it has been previously shown that alpha-Pax6-Cre-mediated inactivation of Numb/Nbl leads to a decrease in RGC production in the retina.[28] A major difference between this previous study and our study is the different onset of expression and cell type specificity of the two different Cre: while Sert-Cre starts to be expressed at E14.5 in committed iRGCs,[15,30] the alpha-Pax6-Cre starts to be expressed at E9 in early retinal progenitors.[37] The later (and iRGC-restricted) expression of the Sert-Cre was important for our study as we wanted to avoid the time window in which Numb/Nbl function is critical for RGC production.

In both iRGC segregation in the visual system and antero-posterior guidance after midline crossing in the spinal cord, Shh plays an important role in inducing growth cone repulsion. We also show that Numb/Nbl also plays a critical role in Shh-mediated iRGC growth cone collapse, directly linking its function in repulsion and the Shh signaling pathway. In addition to the role of Numb/Nbl in Shh-mediated attraction[20] and canonical pathway activation,[38] we now show that Shh-mediated axon repulsion also relies on Numb/Nbl, positioning Numb/Nbl as an

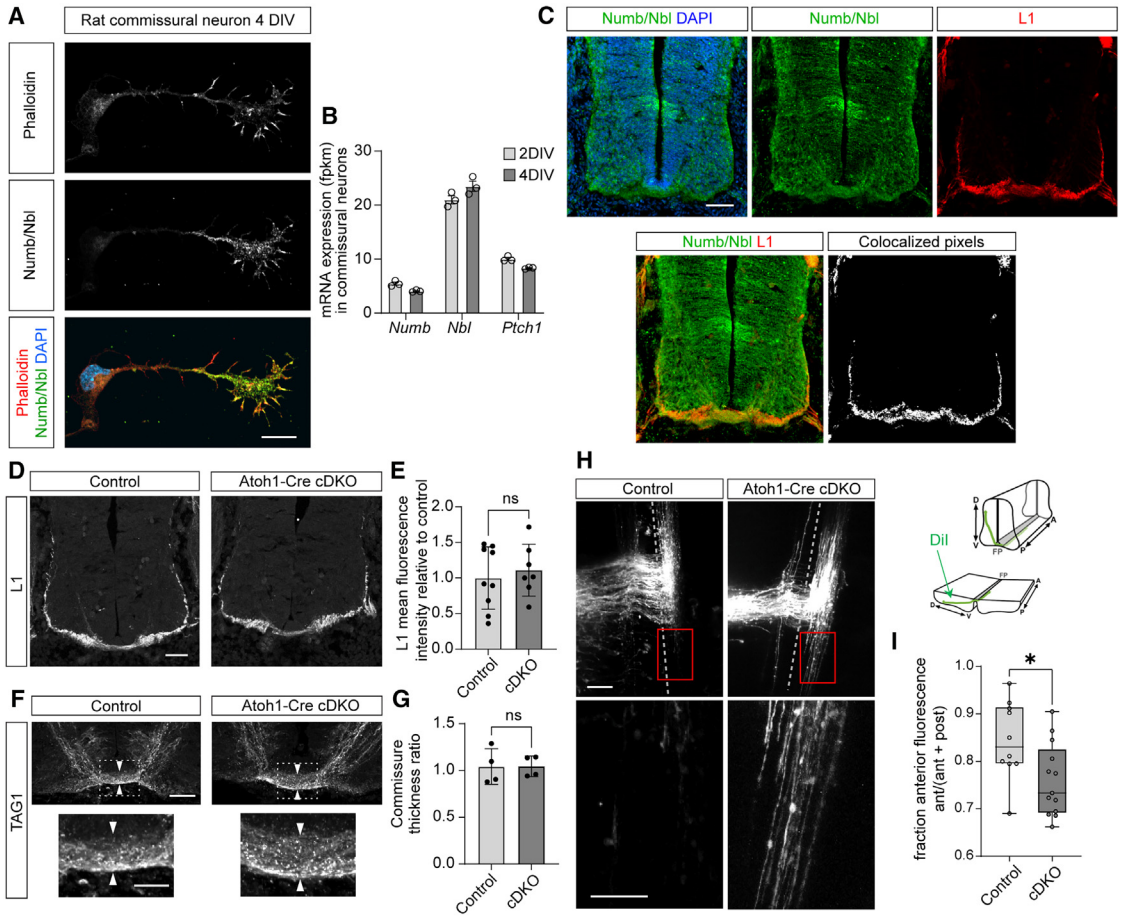

Figure 5. Numb/Nbl is required for post-midline crossing guidance in the developing spinal cord

(A) Rat commissural neurons cultured *in vitro* for 4 days (4 DIV) were immunostained for Numb/Nbl and stained with phalloidin for actin visualization. Nuclei were detected by DAPI.

(B) Mean mRNA expression (fpkm ±s.e.m) of Numb, Nbl, and Ptch1 in dissociated commissural neurons at 2 and 4 DIV (n = 3 independent experiments).

(C) Mouse e11.5 neural tube sections immunostained for Numb/Nbl and L1 to label commissural axons post-crossing.

(D) L1 staining of E11.5 spinal cord sections from control and Atoh1-Cre cDKO.

(E) Mean L1 fluorescence intensity relative to control shows no difference in Atoh1-Cre cDKO mice compared to controls (Data are mean ± s.e.m, Mann-Whitney, dots represent embryos, ns. = not significant: $p > 0.05$).

(F) TAG1 staining of E11.5 spinal cord sections from Atoh1-Cre cDKO and control show ventral commissure morphology.

(G) Commissure thickness is unchanged in Atoh1-Cre cDKO mice compared to controls (Data are mean ± s.e.m, Mann-Whitney, dots indicate embryos dots represent embryos, ns. = not significant: $p > 0.05$).

(H) DiI labeling of post-crossing commissural axons in open book preparations of E12.5 control and Atoh1-Cre cDKO mouse embryos, with magnification of the boxed region. Red boxes indicate magnified areas, vertical dashed lines indicate the midline. Anterior is up.

(I) Relative fluorescence of anterior-directed axons versus total fluorescence of anterior- and posterior-directed axons ($n \geq 10$ embryos per genotype), represented as whisker plots. Mann-Whitney test, dots represent embryos. Asterisks (*) indicate significance as follows: * = $p < 0.05$. Scale bars: 10 μm in (A); 100 μm in (C); 100 μm (top) and 50 μm (bottom) in (F); 50 μm (top) and 25 μm (bottom) in (H). See also Figure S4.

essential component of the Shh signaling pathway in multiple neurodevelopmental functions.

cRGCs also express Numb/Nbl (Figure 1). However, we have not investigated the role of Numb/Nbl in cRGCs. Conditional inactivation of Numb in all RGCs increases tau levels, leading to neurodegeneration and neuronal loss in aged mice, suggesting a critical role for Numb in regulating intracellular tau in all neuronal types at later stages.[32] This suggests that in addition to the axon guidance function that we have identified, Numb/Nbl may also play a role in axon stability and/or growth. However, we did not observe any notable axonal reduction in our embryonic retina explants *in vitro*. It is possible that cRGCs begin to express Numb/Nbl during development but become dependent on it only later.

An intriguing observation of our study is the ability of Numb and Nbl to independently rescue Shh-mediated collapse when both are knocked down (Figure 4). Numb and Nbl are redundant for the maintenance of progenitor cells during early neurogenesis. In many instances, Numb KO has a stronger phenotype than Nbl KO during nervous system development.[23,24] In our

previous study in which we identified Numb/Nbl as an essential Shh signaling component for Shh-mediated attraction, only Numb seemed to be able to rescue their knockdown.[20] This difference suggests that Nbl can rescue Numb deficiency in the context of repulsion but not attraction. This could be related to different requirements of endocytosis between repulsion and attraction, with repulsion being more sensitive to global endocytosis processes. Therefore, overexpressing Nbl could be sufficient in this context whereas its function in attraction may be limited. In fact, at least two types of endocytosis have been reported in neuronal growth cones: clathrin-mediated endocytosis[39] and micropinocytosis.[40,41] Indeed, it has been shown that Shh-induced attraction relies on clathrin-dependent endocytosis of Boc via Numb.[20] On the other hand, Shh-induced growth cone collapse is induced by an upregulation of micropinocytosis mediated by dynamin.[42] Dynamin and clathrin can both bind to the ear domain of α-adaptin, a member of the AP-2 complex that plays an important role in regulating endocytosis.[43,44] Both Numb and Nbl can also associate with α-adaptin,[45] but the difference in rescuing ability of Nbl that we observed in this study might be related to the number of α-adaptin interacting domain in the C-terminus of each protein: Numb has two tripeptide sequences whereas Nbl has only one. Nbl also tends to be less abundant in axons and is located in the perinuclear space whereas Numb is enriched at the plasma membrane.[46] Thus, in the context of repulsion, binding of Nbl to the AP-2 complex may be sufficient to drive micropinocytosis, but not clathrin-mediated endocytosis, which is necessary for attraction.

The identification of endocytic adaptors as essential components of the Shh pathway for multiple and distinct processes, such as axon attraction,[20] repulsion (this study), or cell proliferation,[38] highlights the importance of the internalization process in the pleiotropic functions of Shh. How and where endocytosis should occur is an important question. Indeed, Numb/Nbl has recently been implicated in receptor trafficking within the ciliary pocket.[38] The primary cilium is involved in various Shh-mediated functions. While their role in the canonical Shh signaling pathway is widely accepted,[47,48] their function in axon guidance might depend on the context. Recently, primary cilia have been shown to be required in commissural neurons to modulate receptor transcription, allowing axon repulsion at the floor plate.[49] On the other hand, while the ciliary GTPase Arl13b has been identified as a critical player in Shh-mediated attraction, its localization at primary cilia is not required.[50] This is consistent with the ability of Shh to increase local translation of actin within the growth cone even when the neuronal cell bodies—and thus the primary cilia—are removed.[51] Growth cone collapse is also maintained when axons are severed from the iRGC cell bodies *in vitro*[52]; it would be interesting to also test this in a Shh-mediated repulsion assay. These different observations could be explained by the fact that a direct guidance response to Shh as a pathfinding cue does not require the primary cilium, while a transcriptional response to induce the expression of a receptor requires the primary cilium, akin to canonical Shh signaling. Nonetheless, our study here suggests that endocytosis at the growth cone level remains a common central mechanism for Shh-mediated axon guidance. Overall, the identification of Nb/Nbl as essential components of the Shh pathway in multiple and distinct processes, such as axon attraction,[20] repulsion (this study), and cell proliferation,[38] highlights their fundamental importance in all functions of the Shh pathway.

Limitations of the study

Our study did not identify the molecular mechanism which explains why pre-crossing commissural axons are attracted by Shh while iRGC axons are repelled by Shh. In the future, this will be interesting to determine. In addition, Numb/Nbl may also regulate the trafficking of other axon guidance receptors involved in these axon guidance processes. Further work will be necessary to determine whether Numb/Nbl also function in other signaling pathways.

RESOURCE AVAILABILITY

Lead contact

Further information and requests for resources and reagents should be directed to and will be fulfilled by the lead contact, Julien Ferent (julien.ferent@inserm.fr).

Materials availability

All reagents generated in this study are available upon request to the lead contact.

Data and code availability

- All data reported in this paper will be shared by the lead contact upon request.
- This paper does not report original code.
- Any additional information required to reanalyze the data reported in this paper is available from the lead contact upon request
- The RNA-seq data is publicly available.[35] The accession number is GEO: GSE268644; https://www.ncbi.nlm.nih.gov/geo/query/acc.cgi?acc=GSE268644.

ACKNOWLEDGMENTS

Research performed in the laboratory of J.F. was supported by ATIP-Avenir, Inserm, the Fyssen foundation and a NARSAD Young Investigator Grant from the Brain & Behavior Research Foundation. J.F.'s salary is supported by Inserm and was also supported by the Fondation pour la Recherche Médicale (FRM), FRQS, and CIHR postdoctoral fellowships. The Institut du Fer à Moulin is affiliated with Inserm and Sorbonne University. Research performed in the laboratory of F.C. was supported by funding from the Canadian Institutes of Health Research (CIHR; FDN334023 and PJT180647) and the Canada Foundation for Innovation (33768 and 39794). F.C. holds the Canada Research Chair in Developmental Neurobiology. T.D. was supported by a Fonds de Recherche du Québec – Santé (FRQS) postdoctoral fellowship. We acknowledge the Imaging Platform of Institut du Fer à Moulin for their help in fluorescence imaging. We thank Dr. Carol Mason for providing us with the Zic2 antibody. The 5E1 antibody was obtained from the Developmental Studies Hybridoma Bank developed under the auspices of the NICHD and maintained by the University of Iowa.

AUTHOR CONTRIBUTIONS

Conceptualization: T.D. and J.F.; methodology: T.D., S.B., and J.F.; formal analysis: T.D., S.B., and J.F.; investigation: T.D., S.B., and J.F.; writing—original draft: J.F. and F.C.; supervision: J.F. and F.C.; funding acquisition: J.F. and F.C.

DECLARATION OF INTERESTS

The authors declare no competing interests.

STAR★METHODS

Detailed methods are provided in the online version of this paper and include the following:

- KEY RESOURCES TABLE
- EXPERIMENTAL MODEL AND STUDY PARTICIPANT DETAILS
  - Animals
- METHOD DETAILS
  - Immunostaining
  - DiI tracing
  - CTB tracing
  - Retinal explant cultures and collapse assays
  - Commissural neuron cultures
  - RNAseq data
- QUANTIFICATION AND STATISTICAL ANALYSIS

SUPPLEMENTAL INFORMATION

Supplemental information can be found online at https://doi.org/10.1016/j.isci.2025.112293.

Received: November 25, 2024
Revised: February 12, 2025
Accepted: March 21, 2025
Published: March 26, 2025

REFERENCES

1. Tessier-Lavigne, M., and Goodman, C.S. (1996). The molecular biology of axon guidance. Science *274*, 1123–1133. https://doi.org/10.1126/science.274.5290.1123.
2. Charron, F., Stein, E., Jeong, J., McMahon, A.P., and Tessier-Lavigne, M. (2003). The morphogen sonic hedgehog is an axonal chemoattractant that collaborates with netrin-1 in midline axon guidance. Cell *113*, 11–23. https://doi.org/10.1016/s0092-8674(03)00199-5.
3. Okada, A., Charron, F., Morin, S., Shin, D.S., Wong, K., Fabre, P.J., Tessier-Lavigne, M., and McConnell, S.K. (2006). Boc is a receptor for sonic hedgehog in the guidance of commissural axons. Nature *444*, 369–373. https://doi.org/10.1038/nature05246.
4. Yam, P.T., Langlois, S.D., Morin, S., and Charron, F. (2009). Sonic hedgehog guides axons through a noncanonical, Src-family-kinase-dependent signaling pathway. Neuron *62*, 349–362. https://doi.org/10.1016/j.neuron.2009.03.022.
5. Sauve, R., Morin, S., Yam, P.T., and Charron, F. (2024). beta-arrestins Are Scaffolding Proteins Required for Shh-Mediated Axon Guidance. J. Neurosci. *44*, 2024. https://doi.org/10.1523/JNEUROSCI.0261-24.2024.
6. Balekoglu, N., Michaud, J.F., Sauvé, R., Ayinde, K.S., Lin, S., Liu, Y., Kramer, D.A., Zhang, K., Steffen, A., Stradal, T., et al. (2024). The WAVE regulatory complex interacts with Boc and is required for Shh-mediated axon guidance. iScience *27*, 111333. https://doi.org/10.1016/j.isci.2024.111333.
7. Yam, P.T., Kent, C.B., Morin, S., Farmer, W.T., Alchini, R., Lepelletier, L., Colman, D.R., Tessier-Lavigne, M., Fournier, A.E., and Charron, F. (2012). 14-3-3 proteins regulate a cell-intrinsic switch from sonic hedgehog-mediated commissural axon attraction to repulsion after midline crossing. Neuron *76*, 735–749. https://doi.org/10.1016/j.neuron.2012.09.017.
8. Trousse, F., Martí, E., Gruss, P., Torres, M., and Bovolenta, P. (2001). Control of retinal ganglion cell axon growth: a new role for Sonic hedgehog. Development *128*, 3927–3936. https://doi.org/10.1242/dev.128.20.3927.
9. Williams, S.E., Mann, F., Erskine, L., Sakurai, T., Wei, S., Rossi, D.J., Gale, N.W., Holt, C.E., Mason, C.A., and Henkemeyer, M. (2003). Ephrin-B2 and EphB1 mediate retinal axon divergence at the optic chiasm. Neuron *39*, 919–935. https://doi.org/10.1016/j.neuron.2003.08.017.
10. Fabre, P.J., Shimogori, T., and Charron, F. (2010). Segregation of ipsilateral retinal ganglion cell axons at the optic chiasm requires the Shh receptor Boc. J. Neurosci. *30*, 266–275.
11. Herrera, E., Chedotal, A., and Mason, C. (2024). Development of the Binocular Circuit. Annu. Rev. Neurosci. *47*, 093230. https://doi.org/10.1146/annurev-neuro-111020-093230.
12. Herrera, E., Sitko, A.A., and Bovolenta, P. (2018). Shh-ushing Midline Crossing through Remote Protein Transport. Neuron *97*, 256–258. https://doi.org/10.1016/j.neuron.2018.01.001.
13. Murcia-Belmonte, V., and Erskine, L. (2019). Wiring the Binocular Visual Pathways. Int. J. Mol. Sci. *20*, 3282. https://doi.org/10.3390/ijms20133282.
14. Petros, T.J., Shrestha, B.R., and Mason, C. (2009). Specificity and sufficiency of EphB1 in driving the ipsilateral retinal projection. J. Neurosci. *29*, 3463–3474. https://doi.org/10.1523/JNEUROSCI.5655-08.2009.
15. Peng, J., Fabre, P.J., Dolique, T., Swikert, S.M., Kermasson, L., Shimogori, T., and Charron, F. (2018). Sonic Hedgehog Is a Remotely Produced Cue that Controls Axon Guidance Trans-axonally at a Midline Choice Point. Neuron *97*, 326–340. https://doi.org/10.1016/j.neuron.2017.12.028.
16. Tojima, T., and Kamiguchi, H. (2015). Exocytic and endocytic membrane trafficking in axon development. Dev. Growth Differ. *57*, 291–304. https://doi.org/10.1111/dgd.12218.
17. Winckler, B., and Mellman, I. (2010). Trafficking guidance receptors. Cold Spring Harbor Perspect. Biol. *2*, a001826.
18. Yap, C.C., and Winckler, B. (2012). Harnessing the power of the endosome to regulate neural development. Neuron *74*, 440–451. https://doi.org/10.1016/j.neuron.2012.04.015.
19. Yap, C.C., and Winckler, B. (2015). Adapting for endocytosis: roles for endocytic sorting adaptors in directing neural development. Front. Cell. Neurosci. *9*, 119. https://doi.org/10.3389/fncel.2015.00119.
20. Ferent, J., Giguere, F., Jolicoeur, C., Morin, S., Michaud, J.F., Makihara, S., Yam, P.T., Cayouette, M., and Charron, F. (2019). Boc Acts via Numb as a Shh-Dependent Endocytic Platform for Ptch1 Internalization and Shh-Mediated Axon Guidance. Neuron *102*, 1157–1171. https://doi.org/10.1016/j.neuron.2019.04.003.
21. Salcini, A.E., Confalonieri, S., Doria, M., Santolini, E., Tassi, E., Minenkova, O., Cesareni, G., Pelicci, P.G., and Di Fiore, P.P. (1997). Binding specificity and in vivo targets of the EH domain, a novel protein-protein interaction module. Genes Dev. *11*, 2239–2249. https://doi.org/10.1101/gad.11.17.2239.
22. Zhong, W., Jiang, M.M., Weinmaster, G., Jan, L.Y., and Jan, Y.N. (1997). Differential expression of mammalian Numb, Numblike and Notch1 suggests distinct roles during mouse cortical neurogenesis. Development *124*, 1887–1897. https://doi.org/10.1242/dev.124.10.1887.
23. Petersen, P.H., Zou, K., Hwang, J.K., Jan, Y.N., and Zhong, W. (2002). Progenitor cell maintenance requires numb and numblike during mouse neurogenesis. Nature *419*, 929–934. https://doi.org/10.1038/nature01124.
24. Petersen, P.H., Zou, K., Krauss, S., and Zhong, W. (2004). Continuing role for mouse Numb and Numbl in maintaining progenitor cells during cortical neurogenesis. Nat. Neurosci. *7*, 803–811. https://doi.org/10.1038/nn1289.
25. Nishimura, T., and Kaibuchi, K. (2007). Numb controls integrin endocytosis for directional cell migration with aPKC and PAR-3. Dev. Cell *13*, 15–28. https://doi.org/10.1016/j.devcel.2007.05.003.
26. Zhou, P., Alfaro, J., Chang, E.H., Zhao, X., Porcionatto, M., and Segal, R.A. (2011). Numb links extracellular cues to intracellular polarity machinery to promote chemotaxis. Dev. Cell *20*, 610–622. https://doi.org/10.1016/j.devcel.2011.04.006.
27. Nishimura, T., Fukata, Y., Kato, K., Yamaguchi, T., Matsuura, Y., Kamiguchi, H., and Kaibuchi, K. (2003). CRMP-2 regulates polarized Numb-mediated

endocytosis for axon growth. Nat. Cell Biol. *5*, 819–826. https://doi.org/10.1038/ncb1039.

28. Kechad, A., Jolicoeur, C., Tufford, A., Mattar, P., Chow, R.W.Y., Harris, W.A., and Cayouette, M. (2012). Numb is required for the production of terminal asymmetric cell divisions in the developing mouse retina. J. Neurosci. *32*, 17197–17210. https://doi.org/10.1523/JNEUROSCI.4127-12.2012.
29. Ramamurthy, V., Jolicoeur, C., Koutroumbas, D., Mühlhans, J., Le, Y.Z., Hauswirth, W.W., Giessl, A., and Cayouette, M. (2014). Numb regulates the polarized delivery of cyclic nucleotide-gated ion channels in rod photoreceptor cilia. J. Neurosci. *34*, 13976–13987. https://doi.org/10.1523/JNEUROSCI.1938-14.2014.
30. Koch, S.M., Dela Cruz, C.G., Hnasko, T.S., Edwards, R.H., Huberman, A.D., and Ullian, E.M. (2011). Pathway-specific genetic attenuation of glutamate release alters select features of competition-based visual circuit refinement. Neuron *71*, 235–242. https://doi.org/10.1016/j.neuron.2011.05.045.
31. Wilson, A., Ardiet, D.L., Saner, C., Vilain, N., Beermann, F., Aguet, M., Macdonald, H.R., and Zilian, O. (2007). Normal hemopoiesis and lymphopoiesis in the combined absence of numb and numblike. J. Immunol. *178*, 6746–6751. https://doi.org/10.4049/jimmunol.178.11.6746.
32. Lacomme, M., Hales, S.C., Brown, T.W., Stevanovic, K., Jolicoeur, C., Cai, J., Bois, T., Desrosiers, M., Dalkara, D., and Cayouette, M. (2022). Numb regulates Tau levels and prevents neurodegeneration in tauopathy mouse models. Sci. Adv. *8*, eabm4295. https://doi.org/10.1126/sciadv.abm4295.
33. Herrera, E., Brown, L., Aruga, J., Rachel, R.A., Dolen, G., Mikoshiba, K., Brown, S., and Mason, C.A. (2003). A. Zic2 patterns binocular vision by specifying the uncrossed retinal projection. Cell *114*, 545–557. https://doi.org/10.1016/s0092-8674(03)00684-6.
34. Rebsam, A., Petros, T.J., and Mason, C.A. (2009). Switching retinogeniculate axon laterality leads to normal targeting but abnormal eye-specific segregation that is activity dependent. J. Neurosci. *29*, 14855–14863. https://doi.org/10.1523/JNEUROSCI.3462-09.2009.
35. Makihara, S., Morin, S., Ferent, J., Côté, J.F., Yam, P.T., and Charron, F. (2018). Polarized Dock Activity Drives Shh-Mediated Axon Guidance. Dev. Cell *46*, 410–425. https://doi.org/10.1016/j.devcel.2018.07.007.
36. Matei, V., Pauley, S., Kaing, S., Rowitch, D., Beisel, K.W., Morris, K., Feng, F., Jones, K., Lee, J., and Fritzsch, B. (2005). Smaller inner ear sensory epithelia in Neurog 1 null mice are related to earlier hair cell cycle exit. Dev. Dyn. *234*, 633–650. https://doi.org/10.1002/dvdy.20551.
37. Kammandel, B., Chowdhury, K., Stoykova, A., Aparicio, S., Brenner, S., and Gruss, P. (1999). Distinct cis-essential modules direct the time-space pattern of the Pax6 gene activity. Dev. Biol. *205*, 79–97. https://doi.org/10.1006/dbio.1998.9128.
38. Liu, X., Yam, P.T., Schlienger, S., Cai, E., Zhang, J., Chen, W.-J., Torres Gutierrez, O., Jimenez Amilburu, V., Ramamurthy, V., Ting, A.Y., et al. (2024). Numb positively regulates Hedgehog signaling at the ciliary pocket. Nat. Commun. *15*, 3365. https://doi.org/10.1038/s41467-024-47244-1.
39. Tojima, T., Itofusa, R., and Kamiguchi, H. (2010). Asymmetric clathrin-mediated endocytosis drives repulsive growth cone guidance. Neuron *66*, 370–377. https://doi.org/10.1016/j.neuron.2010.04.007.
40. Fournier, A.E., Nakamura, F., Kawamoto, S., Goshima, Y., Kalb, R.G., and Strittmatter, S.M. (2000). Semaphorin3A enhances endocytosis at sites of receptor-F-actin colocalization during growth cone collapse. J. Cell Biol. *149*, 411–422. https://doi.org/10.1083/jcb.149.2.411.
41. Kabayama, H., Nakamura, T., Takeuchi, M., Iwasaki, H., Taniguchi, M., Tokushige, N., and Mikoshiba, K. (2009). Ca2+ induces macropinocytosis via F-actin depolymerization during growth cone collapse. Mol. Cell. Neurosci. *40*, 27–38. https://doi.org/10.1016/j.mcn.2008.08.009.
42. Kolpak, A.L., Jiang, J., Guo, D., Standley, C., Bellve, K., Fogarty, K., and Bao, Z.Z. (2009). Negative guidance factor-induced macropinocytosis in the growth cone plays a critical role in repulsive axon turning. J. Neurosci. *29*, 10488–10498. https://doi.org/10.1523/JNEUROSCI.2355-09.2009.
43. Berdnik, D., Török, T., González-Gaitán, M., and Knoblich, J.A. (2002). The endocytic protein alpha-Adaptin is required for numb-mediated asymmetric cell division in Drosophila. Dev. Cell *3*, 221–231. https://doi.org/10.1016/s1534-5807(02)00215-0.
44. Shin, J., Nile, A., and Oh, J.W. (2021). Role of adaptin protein complexes in intracellular trafficking and their impact on diseases. Bioengineered *12*, 8259–8278. https://doi.org/10.1080/21655979.2021.1982846.
45. Santolini, E., Puri, C., Salcini, A.E., Gagliani, M.C., Pelicci, P.G., Tacchetti, C., and Di Fiore, P.P. (2000). Numb is an endocytic protein. J. Cell Biol. *151*, 1345–1352. https://doi.org/10.1083/jcb.151.6.1345.
46. Shao, X., Liu, Y., Yu, Q., Ding, Z., Qian, W., Zhang, L., Zhang, J., Jiang, N., Gui, L., Xu, Z., et al. (2016). Numb regulates vesicular docking for homotypic fusion of early endosomes via membrane recruitment of Mon1b. Cell Res. *26*, 593–612. https://doi.org/10.1038/cr.2016.34.
47. Andreu-Cervera, A., Catala, M., and Schneider-Maunoury, S. (2021). Cilia, ciliopathies and hedgehog-related forebrain developmental disorders. Neurobiol. Dis. *150*, 105236. https://doi.org/10.1016/j.nbd.2020.105236.
48. Ingham, P.W. (2022). Hedgehog signaling. Curr. Top. Dev. Biol. *149*, 1–58. https://doi.org/10.1016/bs.ctdb.2022.04.003.
49. Dumoulin, A., Wilson, N.H., Tucker, K.L., and Stoeckli, E.T. (2024). A cell-autonomous role for primary cilium-mediated signaling in long-range commissural axon guidance. Development *151*, dev202788. https://doi.org/10.1242/dev.202788.
50. Ferent, J., Constable, S., Gigante, E.D., Yam, P.T., Mariani, L.E., Legué, E., Liem, K.F., Jr., Caspary, T., and Charron, F. (2019). The Ciliary Protein Arl13b Functions Outside of the Primary Cilium in Shh-Mediated Axon Guidance. Cell Rep. *29*, 3356–3366. https://doi.org/10.1016/j.celrep.2019.11.015.
51. Lepelletier, L., Langlois, S.D., Kent, C.B., Welshhans, K., Morin, S., Bassell, G.J., Yam, P.T., and Charron, F. (2017). Sonic Hedgehog Guides Axons via Zipcode Binding Protein 1-Mediated Local Translation. J. Neurosci. *37*, 1685–1695. https://doi.org/10.1523/JNEUROSCI.3016-16.2016.
52. Campbell, D.S., and Holt, C.E. (2001). Chemotropic responses of retinal growth cones mediated by rapid local protein synthesis and degradation. Neuron *32*, 1013–1026. https://doi.org/10.1016/s0896-6273(01)00551-7.
53. Gong, S., Doughty, M., Harbaugh, C.R., Cummins, A., Hatten, M.E., Heintz, N., and Gerfen, C.R. (2007). Targeting Cre recombinase to specific neuron populations with bacterial artificial chromosome constructs. J. Neurosci. *27*, 9817–9823. https://doi.org/10.1523/JNEUROSCI.2707-07.2007.
54. Zilian, O., Saner, C., Hagedorn, L., Lee, H.Y., Säuberli, E., Suter, U., Sommer, L., and Aguet, M. (2001). Multiple roles of mouse Numb in tuning developmental cell fates. Curr. Biol. *11*, 494–501. https://doi.org/10.1016/s0960-9822(01)00149-x.
55. Madisen, L., Zwingman, T.A., Sunkin, S.M., Oh, S.W., Zariwala, H.A., Gu, H., Ng, L.L., Palmiter, R.D., Hawrylycz, M.J., Jones, A.R., et al. (2010). A robust and high-throughput Cre reporting and characterization system for the whole mouse brain. Nat. Neurosci. *13*, 133–140. https://doi.org/10.1038/nn.2467.
56. Plump, A.S., Erskine, L., Sabatier, C., Brose, K., Epstein, C.J., Goodman, C.S., Mason, C.A., and Tessier-Lavigne, M. (2002). Slit1 and Slit2 cooperate to prevent premature midline crossing of retinal axons in the mouse visual system. Neuron *33*, 219–232. https://doi.org/10.1016/s0896-6273(01)00586-4.
57. Farmer, W.T., Altick, A.L., Nural, H.F., Dugan, J.P., Kidd, T., Charron, F., and Mastick, G.S. (2008). Pioneer longitudinal axons navigate using floor plate and Slit/Robo signals. Development *135*, 3643–3653. https://doi.org/10.1242/dev.023325.
58. Jaubert-Miazza, L., Green, E., Lo, F.S., Bui, K., Mills, J., and Guido, W. (2005). Structural and functional composition of the developing

retinogeniculate pathway in the mouse. Vis. Neurosci. *22*, 661–676. https://doi.org/10.1017/S0952523805225154.

59. Muir-Robinson, G., Hwang, B.J., and Feller, M.B. (2002). Retinogeniculate axons undergo eye-specific segregation in the absence of eye-specific layers. J. Neurosci. *22*, 5259–5264. https://doi.org/10.1523/JNEUROSCI.22-13-05259.2002.
60. Torborg, C.L., and Feller, M.B. (2004). Unbiased analysis of bulk axonal segregation patterns. J. Neurosci. Methods *135*, 17–26. https://doi.org/10.1016/j.jneumeth.2003.11.019.
61. Langlois, S.D., Morin, S., Yam, P.T., and Charron, F. (2010). Dissection and culture of commissural neurons from embryonic spinal cord. J. Vis. Exp. 1773. https://doi.org/10.3791/1773.

STAR★METHODS

KEY RESOURCES TABLE

REAGENT or RESOURCE	SOURCE	IDENTIFIER
Antibodies		
Anti-Zic2	Gift from Dr C. Mason	N/A
Rabbit anti-Numb/NumbLike	Abcam	Cat# ab14140 lot #GR3400275-3 RRID: AB_443023
Rabbit anti-Numb/NumbLike (C29G11)	Cell Signaling Technology	Cat# 55673 lot #5 RRID: AB_2799493
Mouse anti-βIII-tubulin	Abcam	Cat# ab18207, lot #1056145-1 RRID: AB_444319
Goat Contactin-2/TAG1 Antibody	R&D Systems	Cat# AF4439, lot # RRID: AB_2044647
Mouse anti-Shh	Developmental Studies Hybridoma Bank	Cat# 5E1 RRID: AB_528466
Rat Anti-L1	Millipore	Cat# MAB5272 lot # RRID: AB_2133200
Goat Anti-SERT	Santa Cruz Biotechnology	Cat# sc-1458 Lot# RRID: AB_632391
Chicken anti-GFP	Aves Labs	Cat# GFP1202 Lot#GFP917979 RRID: AB_2734732
Donkey Anti-Chicken IgY (IgG) (H + L) 488	Jackson ImmunoResearch Labs	Cat# 703-546-155 Lot#703-546-155 RRID: AB_2340376
Donkey Anti-Goat IgG (H&L) 594	Abcam	Cat# ab150132 Lot#1005774-1 RRID: AB_2810222
Donkey Anti-Mouse IgG (H + L) Cy5	Jackson ImmunoResearch Labs	Cat# 715-175-150 Lot#715-606-150 RRID: AB_2340819
Phalloidin-TRITC	Sigma-Aldrich	Cat# P1951 Lot# RRID: AB_2315148
Donkey anti-rabbit IgG 488	Jackson ImmunoResearch Laboratory	Cat#: 711-545-152; Lot#711-546-152 RRID: AB_2313584
Bacterial and virus strains		
DH5α	Life Technologies	Cat#: 18265-017
Biological samples		
Mouse retinal explants	This manuscript	N/A
Rat spinal commissural neurons	This manuscript	N/A
Chemicals, peptides, and recombinant proteins		
SHH C24II	R&D systems	Cat# 1845-SH
DMEF12	Thermofisher Scientific	Cat# 21331
Bovine Serum Albumin	Sigma-Aldrich	Cat# A1933 CAS No 9048-46-8
Supplement B-27	ThermoFisher Scientific	Cat# 17504044
L-Glutamine	ThermoFisher Scientific	Cat# 25030081
Penicillin/Streptomycin/Amphotericin B	Cytiva	Cat# SV30079.01

(*Continued on next page*)

Continued

REAGENT or RESOURCE	SOURCE	IDENTIFIER
Laminin	Sigma-Aldrich	Cat# L2020 CAS No 114956-81-9
Methyl cellulose	Sigma-Aldrich	Cat#M7027
Poly-L-Lysine (molecular weight ≥300,000)	Sigma-Aldrich	Cat# P1524
Poly-L-lysine solution (molecular weight 70,000–150,000, concentration: 0.01%)	Sigma-Aldrich	Cat# P4707
DiI crystals	Thermo Fisher Scientific	Cat# D282
Cholera Toxin Subunit B (Recombinant), Alexa Fluor™ 594 Conjugate	ThermoFisher Scientific	Cat# C34777
Cholera Toxin Subunit B (Recombinant), Alexa Fluor™ 488 Conjugate	ThermoFisher Scientific	Cat# C22841
DAPI	Sigma-Aldrich	Cat# D95964
Deposited data		
Commissural neuron RNAseq dataset	Makihara et al.[35]	GSE268644; https://www.ncbi.nlm.nih.gov/geo/query/acc.cgi?acc=GSE268644
Experimental models: Organisms/strains		
Mus musculus C57BL/6JRj	Janvier Labs	RRID:MGI:2670020
Mouse: Tg(Atoh1-cre)1Bfri	The Jackson Laboratory (Matei et al.[36])	RRID:IMSR_JAX:011104
Mouse: Slc6a4 (ET33-SERT)-Cre	Mutant Mouse Resource and Research Center (MMRRC)	RRID:MMRRC_031028-UCD:
Mouse: Numb^{tm1Zili}/Numbl^{tm1Zili}	The Jackson Laboratory (Wilson et al.[31])	RRID:IMSR_JAX:005384
Mouse: B6.Cg-Gt(ROSA)26Sor$^{tm14(CAG–tdTomato)Hze}$/J	Obtained from the colony of Y. Zhang (Dalhousie University)	RRID:IMSR_JAX:007914
Recombinant DNA		
shRNA Numb (pCAGGS -GW/EmGFP-miR *Numb*)	Ferent et al.[20]	N/A
shRNA Numblike (pCAGGS -GW/EmGFP-miR *Numblike*)	Ferent et al.[20]	N/A
Numb resistant (pCAGGS-Rat Numb (shRNA-resistant))	Ferent et al.[20]	N/A
Numblike resistant (pCAGGS-Rat Numblike (shRNA-resistant))	Ferent et al.[20]	N/A
Software and algorithms		
ImageJ	NIH	https://imagej.nih.gov/ij/; RRID:SCR_003070
GraphPad Prism	GraphPad Software Inc.	RRID:SCR_002798
Metamorph	Molecular Devices	https://www.moleculardevices.com/products/cellular-imaging-systems/acquisition-and-analysis-software/metamorph-microscopy
Illustrator CC	Adobe	https://www.adobe.com/fr/
Photoshop CC	Adobe	https://www.adobe.com/fr/
Other		
Electroporation paddles	Sonidel	CUY650P5
Electroporator ECM830	BTX	Cat 45-0662

EXPERIMENTAL MODEL AND STUDY PARTICIPANT DETAILS

Animals

Animal work was performed in accordance with the Canadian Council on Animal Care Guidelines and approved by the IRCM Animal Care Committee. Staged pregnant Sprague-Dawley rats were obtained from Charles River (St. Constant, Canada) and staged pregnant wild type mice used for explants were obtained from Janvier labs (France). Transgenic mice were maintained in the IRCM

specific pathogen-free animal facility. For *in vitro* assays from mouse embryos, research was carried out conforming to national and international directives (directive CE 2010/63/EU, French national APAFIS#3 0246–2021030513285313 v3) with protocols followed and approved by the local ethical committee (Charles Darwin, Paris, France). All mouse lines have been previously described: Atoh1-Cre,[36] Slc6a4 (ET33-SERT)-Cre ([53], obtained from the Mutant Mouse Regional Resource Center (MMRRC) of UC Davis), Numb conditional allele and NumbLike conditional allele ([31,54], obtained from The Jackson Laboratory), ROSA26-tdTomato ([55], kindly provided by Dr. Ying Zhang at the Dalhousie University). When ROSA26-tdTomato was used, control genotype is Sert-cre; $Nb^{lox/+}$; $Nbl^{lox/lox}$. Embryonic day 0 (E0) was defined as midnight of the night before a plug was found. Males and females were used in all analyses.

METHOD DETAILS

Immunostaining

Postnatal day 0 (P0) eyes sections were stained with anti-Zic2 (a kind gift from C. Mason). Embryo sections were immunostained with anti-Numb/NumbLike antibody (Abcam, ab14140 or Cell Signaling Technology, #2756), anti-Tag-1 (R&D Systems, AF4439) and anti-L1 (Chemicon MAB5272). Retinal explants were permeabilized and blocked with 0.25% (v/v) Triton and 3% (w/v) BSA in PBS, then immunostained with antibodies against: GFP (Aves Labs, GFP1020) followed by a secondary antibody coupled to Alexa Fluor 488 (Jackson ImmunoResearch), SERT (Santa-Cruz, sc-1458) followed by a secondary antibody coupled to Alexa Fluor 594 (Abcam), and βIII-tubulin (Abcam, ab18207) followed by a secondary antibody coupled to Cy5 (Jackson ImmunoResearch). Antibodies were diluted in PBS supplemented with 0.1% (v/v) Triton and 1% (w/v) BSA. Dissociated rat commissural neurons were immunostained with anti-Numb/NumbLike antibody (Abcam, ab14140). Filamentous actin was detected with phalloidin (Sigma, P1951).

DiI tracing

For iRGC projection measurement in the optic tract, mono-ocular DiI crystals-filling of the retina was performed at P0 on fixed tissue, as previously described.[10,56] After allowing the dye to diffuse, 30 μm-thick coronal sections just caudal to the optic chiasm were performed and the amount of DiI fluorescence signal was quantified in the contralateral and ipsilateral optic tracts. All images were acquired under conditions where the pixels were not saturated using a Leica DM4000 microscope (Leica Microsystems GmbH, Wetzlar, Germany) and an Orca ER CCD camera (Hamamatsu Photonics, Hamamatsu City, Japan). Fluorescence measurements were taken blind to the genotype on ten consecutive sections per animal using Volocity version 4.3 (Improvision, Waltham, MA, USA). The ipsilateral index was calculated by dividing the fluorescent intensity in the ipsilateral optic tract by the sum of the fluorescent intensity in ipsilateral + contralateral optic tracts.

For the post-crossing guidance assay in the spinal cord, the neural tubes were dissected from E12.5 embryos and fixed at least overnight at 4°C in 4% paraformaldehyde in PBS. After fixation, a small amount of 1,1′-dioctadecyl-3,3,3′,3′-tetramethylindocarbocyanine perchlorate (DiI, Molecular Probes, Eugene, OR) dissolved in ethanol (10 mg/ml) was inserted to the medial neural tube dorsal of the motor column to label several individual cohorts per embryo (around 5–9) at multiple levels along the AP axis.[57] The DiI was allowed to diffuse for 2 days at 4°C. After diffusion of the dye, the neural tubes were mounted in an open-book configuration and imaged on a confocal microscope (Leica LSM700). Analysis of axon guidance and image processing was performed on the resulting Z-stacks in ImageJ (NIH). Analyses were performed blind to the genotype. All images shown are maximum projections of the Z-stacks.

CTB tracing

Anterograde cholera toxin B subunit (CTB) labeling was performed as previously described.[34,58] Briefly, adult mice were deeply anesthetized with a mixture of isoflurane (5% for induction and 2% for maintenance) and a 1:1 flow ratio of air/O2 (1 L/min). Eyes were injected with a glass pipette intravitreally with 5μL of 0.2% CTB conjugated to Alexa Fluor 594 or 488 (Invitrogen by Life Technology, Carlsbad, CA, USA) diluted in 1% DMSO. After 3 days, mice were anesthetized and perfused with 4% PFA in 0.1 M PB before dissection of brain and retinas. Brains were post-fixed overnight, embedded in 4% agarose, and sectioned (80 μm) with a Leica VT1000S vibratome. Coronal sections were directly mounted in Mowiol and imaged on a confocal microscope (Leica LSM700). As Alexa Fluor 594-labeled contralateral/Alexa Fluor 488-labeled ipsilateral projections had a better signal-to-noise ratio, the analyses were conducted on these images, as already described.[34,59,60] Quantification was performed on z stack images from three consecutive coronal sections through the region of the dLGN containing the greatest extent of the ipsilateral projections. For this, the boundary of the dLGN was delineated in order to exclude label from the intrageniculate leaflet, the ventral lateral geniculate nucleus, and the optic tract. Analyses were performed blind to the genotype. Using ImageJ software (NIH), the proportion of dLGN occupied by ipsilateral axons was quantified as a ratio of ipsilateral pixels to the total number of pixels in the dLGN region using a multi-threshold analysis. This analysis was developed in Dr. Carol Mason's lab (see details in[34]).

Retinal explant cultures and collapse assays

Retinas of E14.5 mouse embryos were electroporated with Numb and Numb-like or scramble shRNA (1 $\mu g\ \mu l^{-1}$ for each plasmid) using 5 pulses of 45 V during 50 ms every 950 ms with an ECM 830 square wave electroporator (BTX). shNb, shNbl, as well as the shRNA-resistant Numb and Nbl expression vectors have been previously validated in our hands.[20] Retinas were dissected and kept 24 h in culture medium (DMEM-F12 supplemented with 1 mM glutamine (Sigma Aldrich), 1% penicillin/streptomycin/AmphotericinB (Cytiva), 0.001% BSA (Sigma Aldrich) and 0.07% glucose), in a humidified incubator at 37°C and 5% CO2. The following day, the retinas were cut

into 200 μm squares with a razorblade and explants were plated on glass coverslips coated with 100 μg ml^{-1} poly-lysine and 20 μg ml^{-1} laminin (Sigma Aldrich). Cells were cultured for 24 h in culture medium supplemented with 0.5% (w/v) methylcellulose and B-27 (1/50, Life technologies). Retinal explants were treated with 240 ng ml^{-1} SHH C24II (R&D Systems, 1845-SH) for 30 min before fixation with 4% (w/v) PFA in PBS for 30 min.

Commissural neuron cultures

Spinal commissural neurons were dissected from rat embryos and cultured as described previously.[61] Briefly, the dorsal fifth of e13 rat neural tubes were microdissected and trypsinized in 0.15% trypsin in Ca2+/Mg2+-free HBSS for 7 min at 37°C. DNase was added briefly. The tissue fragments were then washed and triturated in Ca2+/Mg2+-free HBSS to yield a suspension of single cells. Cells were plated in Neurobasal media supplemented with 10% heat-inactivated FBS and 2 mM GlutaMAX. After ∼21 h, the medium was changed to Neurobasal supplemented with 2% B27 and 2 mM GlutaMAX. Commissural neurons were used for experiments either at ∼48 h after plating (DIV2) or 36 to 48 h after plating (DIV4).

RNAseq data

We analyzed RNAseq data previously generated in our lab.[35] The dataset is available via GEO: GSE268644.

QUANTIFICATION AND STATISTICAL ANALYSIS

Statistical analyses were performed with GraphPad Prism 10 (La Jolla, CA). Mann-Whitney's test were used when there were two groups in the dataset. To compare multiple groups in a dataset, one- or two-way ANOVA was used. Kruskal-Wallis was used as a non-parametric alternative to the one-way ANOVA test. The statistical analysis used in each experiment and the definition of n are stated in the figure legends. Asterisks (*) indicate significance as follows: * = $p < 0.05$, ** = $p < 0.01$, *** = $p < 0.001$, **** = $p < 0.0001$, n.s. = not significant ($p > 0.05$).